that the validity of the hydrodynamic equation in the selvage region is still open to question. What we have shown is that independent of what happens in the selvage region, the hydrodynamic equation with a boundary condition on the current and with β given by Fig. 1 has solutions which outside the selvage region are identical to solutions of the Boltzmann equation with a particular microscopic boundary condition. Undoubtedly, the hydrodynamic equation could be further refined to make it more valid in the selvage region by making β a function of position as well as of frequency.

ACKNOWLEDGMENTS

The author wishes to thank Professor Robert Swenson and the Physics Department of Montana State University for their hospitality during the NSF sponsored 1972 Summer Physics Workshop.

*Research supported by the Air Force Office of Scientific Research (AFSC) under Grant Nos. AF-AFOSR-68-1507 and AF-AFOSR-72-2308.

[1]P. J. Feibelman, C. B. Duke, and A. Bagchi, Phys. Rev. B **5**, 2436 (1972).
[2]D. M. Newns, Phys. Rev. B **1**, 3304 (1970).
[3]P. J. Feibelman, Phys. Rev. **176**, 551 (1968).
[4]D. E. Beck and V. Celli, Phys. Rev. Lett. **28**, 1124 (1972).
[5]Although Beck and Celli used wave functions calculated from a finite-potential-wall model, they used an overly simple variational function which forced $n_1(z)=0$ for $z<0$.
[6]A. J. Bennett, Phys. Rev. B **1**, 203 (1970).
[7]J. Harris, Phys. Rev. B **4**, 1022 (1971).
[8]D. Wagner, Z. Naturforsch. A **21**, 634 (1966).
[9]R. H. Ritchie, Prog. Theor. Phys. **29**, 607 (1963).
[10]See Eq. (29) of Ref. 8.
[11]This is Bennett's Eq. (3.2) (see Ref. 6).

PHYSICAL REVIEW B VOLUME 7, NUMBER 6 15 MARCH 1973

Electric Field Gradients in Dilute Copper Alloys*

George Schnakenberg, Jr.† and R. T. Schumacher
Department of Physics, Carnegie-Mellon University, Pittsburgh, Pennsylvania 15213
(Received 29 September 1972)

The electric-quadrupole-tensor parameters of copper neighbors to the impurities Zn, Cd, Ag, and Au have been measured by studying the angular dependence of the second-order splitting of the $\frac{1}{2} \leftrightarrow -\frac{1}{2}$ nuclear-magnetic-resonance transitions in single crystals of copper metal. The parameters for the first neighbors were determined for all the impurities, and for the second neighbors to Cd, Ag, and Au. The results for the charged impurities complement the work of Jensen, Nevald, and Williams on Ge, In, Sn, and Sb in copper, and show a systematic change in the electric field gradient at nearest-neighbor sites as a function of impurity valence for which present theory is inadequate.

I. INTRODUCTION

Electric field gradients in metals have been studied by nuclear magnetic resonance with basically two types of experiments. The gross long-range disturbance of the conduction-electron system caused by the impurity is measured by the NMR-intensity-change-vs-concentration experiments, such as in the studies by Rowland[1] on a great variety of solutes in the copper matrix. Considerable theoretical work on the screening of the excess impurity charge by the conduction electrons of the host was stimulated by Rowland's experiments, and a reasonably quantitative agreement between experiment and theory has been achieved. About ten years ago Redfield[2] measured the zero-field pure quadrupole resonance of copper neighbors of Zn and Ag impurities by a double-resonance technique. His was the first specific determination of the strength of the nuclear-electric-quadrupole interaction at some particular site relative to the impurity. However, because his experiment was on a powdered sample, he could not determine which nuclear sites were responsible for the resonances he observed, nor could he identify the orientation of the axes of the electric-field-gradient (efg) tensor, or the magnitude of the asymmetry parameter η.

High-magnetic-field single-crystal studies do allow determination of these other aspects of the electric-quadrupole interaction. The first such experiment was reported on the Cu-Zn system by the present authors,[3] and the present report represents an extension and completion of that work. Meanwhile, Jensen, Nevald, and Williams[4] have completed a similar study on copper single crystals with the charged impurities In, Sn, Sb, and Ge. Our results on the charged impurities Zn and Cd will be seen to complement theirs, and support the systematic result which was evident from their data. Our results on the systems with the monovalent impurities Ag and Au, on the other hand, do

not fit into the pattern suggested by the multivalent impurities, and presumably will have to be understood in a rather different framework. In either event, the theoretical picture developed in the context of the "wipeout-number" experiments is clearly, and not unexpectedly, inapplicable to nearest neighbors.

In Sec. II of this paper we briefly describe some experimental details and the method of analysis of the data. In Sec. III we summarize all the known data and present some tentative suggestions for their explanation.

II. EXPERIMENTAL

(*a*) *Samples.* The sample were made from a single crystal of pure copper (more than 99.9999% pure) obtained from Metal Research Instrument Corporation (Monsey, N. Y.) in the form of a cylinder $\frac{1}{4}$-in. diam by 6 in. long. A [110] crystal axis was parallel to the cylinder axis. The original crystal was spark cut into cylinders approximately 1 in. long, and the impurities diffused in from the surface by heating the sample in an atmosphere of the desired impurity atoms. Since the nuclear-magnetic-resonance signal is due only to nuclei in the rf skin depth, it was sufficient to allow the process to continue only long enough to obtain the desired concentration of impurity in the first 50–100 μm of the cylindrical surface. The concentrations were measured by electron microprobe.

The details of the sample preparation are summarized in Table I. The impurities divide themselves into two groups for the purpose of sample preparation. Zinc and cadmium are high-vapor-pressure metals. To obtain the desired concentration on the surface of the sample, the solutes Zn and Cd were supplied from donor alloys (column 2 of Table I) which were placed near the copper single crystal in an evacuated quartz ampule. The low-vapor-pressure impurities Ag and Au were handled differently: Ag was placed in the pure state inside the ampule while Au was electrochemically deposited onto the surface of the copper. The third and fourth columns show the preparation conditions and the last two columns show the results of the electron-microprobe analysis on a piece of the sample spark cut from one end, prepared for microprobe analysis, and scanned radially inward from the edge at several spots. The last column shows the depth to which the indicated concentration extended with reasonable uniformity.

(*b*) *Apparatus.* The samples were tightly wound with about 70 turns of 0.005-in. silver wire covered with 0.001-in. -thick Teflon insulation. The windings occupied the center two-thirds of the sample. The sample and coil formed part of the tank circuit of a Robinson NMR oscillator which was operated between 2 and 14 MHz. Most of the data were taken at constant magnetic field (provided by a 12-in. Varian electromagnet with 6-in. tapered pole caps) puls small modulating field, with the frequency of the Robinson oscillator slowly swept by about 200 kHz about the pure Cu^{63} resonance frequency. The signal was detected by standard lock-in detection and the demodulated signal recorded on a strip-chart recorder on which frequency markers were made manually by visually monitoring a frequency counter connected to the Robinson oscillator. Some data were taken by repetitiously sweeping the field and storing the lock-in output in a Fabritek 1070 signal averager. This field-sweep method was good for finding the weakest signals: In general, however, data analysis is harder when the external field is being changed, since the nuclear spin Hamiltonian is being changed in the course of the experiment by an amount which is not wholly insignificant.

(*c*) *Data analysis.* The nuclear spin Hamiltonian may be written

$$\mathcal{H}=\gamma_N \hbar B_0 I_{z'}+\frac{e^2qQ}{4I(2I-1)}[3I_z^2-I(I+1)+\eta(I_x^2-I_y^2)], \tag{1}$$

where eQ is the nuclear-quadrupole moment and the z direction is the direction of the largest efg component in its principal-axis system, $eq=V_{zz}$. If the x and y directions are chosen so that $|V_{zz}|>|V_{yy}|>|V_{xx}|$, the asymmetry parameter

$$\eta=(V_{xx}-V_{yy})/V_{zz} \tag{2}$$

satisfies $0\leq\eta\leq1$, since (1) has been written so that the efg tensor is traceless. The external field is applied in the z' direction, which makes an angle θ with the z axis.

TABLE I. Summary of sample preparation treatments and results.

Solute	Donor form or alloy concentration	Diffusion temperature (°C)	Diffusion time (h)	Atomic percent concentration	Depth (μm)
Zn	5 at.%	900	18	1.5–1.0	>40
Cd	1.75 at.%	900	24	0.7	>180
Ag	Ag shot	950	127	0.65	>250
Ag	Ag wire	950	48	1.2	
Au	Au film	850	62	0.75	~50

TABLE II. Second-order frequency shift of the central transitions for the first- and second-nearest neighbors to the solute. The magnetic field is in the (011) plane at an angle θ from the $[01\bar{1}]$ direction. $A = e^2qQ/2h$ and $\mu = \cos\theta$.

First-nearest-neighbor sites	
$\pm(0,1,1)$	$\Delta\nu = \frac{A}{\nu_L}[\eta^2(1-9\sin^2 2\theta)+6\eta\cos 2\theta+9]$.
$\pm(0,\bar{1},1)$	$\Delta\nu = \frac{A}{\nu_L}[9(1-\mu^2)(1-9\mu^2)-6\eta(1-\mu^2)(1+9\mu^2)+\eta^2(1-3\mu^2)^2]$.
$\pm(1,1,0)$ and $\pm(1,0,1)$	$\Delta\nu = \frac{A}{\nu_L}(\frac{1}{16}\{[3(\eta+1)\cos^2\theta+2\sqrt{2}(\eta-3)\cos\theta\sin\theta]^2 + [6(\eta+1)\sin\theta+2\sqrt{2}(\eta-3)\cos\theta]^2\} - \frac{1}{2}\{[\sqrt{2}(\eta-3)(\cos^2\theta-\sin^2\theta)-3(\eta+1)\sin\theta\cos\theta]^2 + [\sqrt{2}(\eta-3)\sin\theta-3(\eta+1)\cos\theta]^2\})$.
$\pm(1,1,0)$ and $\pm(1,0,1)$	Change θ to $-\theta$ in the preceding formula for the $\pm(1,1,0)$ pair.
Second-nearest-neighbor sites	
$(0,0,1)$ and $(0,1,0)$	$\Delta\nu = \frac{A}{\nu_L}[9(1-\frac{1}{2}\cos^2\theta)(1-\frac{9}{2}\cos^2\theta)]$.
$(1,0,0)$	$\Delta\nu = \frac{A}{\nu_L}[9(1-\sin^2\theta)(1-9\sin^2\theta)]$.

In our case, the magnetic field was chosen to rotate about the [011] crystalline axis. The angular dependence of the second-order splitting of the $\frac{1}{2} \rightarrow -\frac{1}{2}$ transition is shown in Table II for the 12 nearest neighbors, at (011)-type positions relative to the impurity at (000), and for the six next-nearest neighbors, at (100)-type sites, for which $\eta = 0$ by symmetry. Table II has been calculated assuming that for the nearest neighbor at (011), for example, the z direction is in the [011] direction. As the table indicates, however, because the resonances from that nucleus and its mirror image in the [010] plane have the same angular dependence, it is not possible to choose between [011] and $[0\bar{1}1]$ for the principal axis of the efg.

The angular dependences of the satellite lines were fitted to the appropriate expressions in Table II using a least-squares adjustment of the parameters A, ν_L, and η. The Larmor frequency ν_L was included among the adjustable parameters to allow for the possibility that the Knight shift of nuclei near the solute need not be the same as for the nuclei far from the solvent, which contribute to the large principal resonance. The results of our measurements are presented in Table III, along with the results of Jensen *et al.*[4] The results of the Knight shift, or ν_L measurement, are not included since the measured Knight shift was within ±3% (our measurement accuracy) of the bulk Knight shift for copper.

Discussion

Charged Solutes

Nearest neighbors. Inspection of Table III, excepting the noble-metal solutes, reveals immediately the systematic result for nearest neighbors

TABLE III. e^2qQ/h (in MHz) and asymmetry parameter η for nearest and next-nearest(nn) neighbors of impurities in copper.

Excess charge	0	1	2	3	4
Solute	Copper host	Zinc	Gallium	Germanium[a]	Arsenic[a]
First nn $e^2qQ/2h$	···	1.96	···	1.94	···
First nn η	···	0.265	···	0.9	···
Second nn $e^2qQ/2h$	···	0.090[b]	···	<0.8	···
Wipe-out number[c]	···	18	38	63	80
Solute	Silver	Cadmium	Indium[a]	Tin[a]	Antimony[a]
First nn $e^2qQ/2h$	0.57	1.52	2.22	2.3	2.6
First nn η	0.75	0.036	0.32	0.64	0.75
Second nn $e^2qQ/2h$	0.475	0.41	<0.8	1.16	1.74
Wipe-out number	25	32	48	67	87
Solute	Gold				
First nn $e^2qQ/2h$	2.65				
First nn η	0.05				
Second nn $e^2qQ/2h$	0.823				
Wipe-out number	44				

[a]Jensen *et al.*, Ref. 4. [b]Redfield, Ref. 2. Site assignment not confirmed. [c]Rowland, Ref. 1.

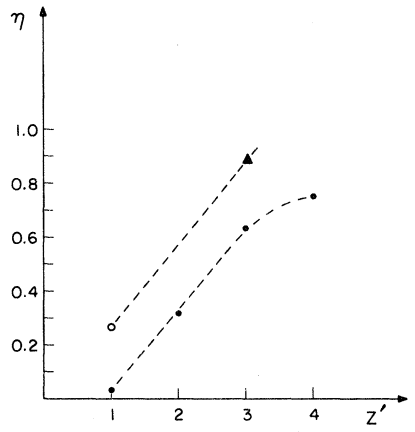

FIG. 1. Asymmetry parameter η as a function of excess valence charge Z'. ○, Zn; ▲, Ge; ●, Cd; row of periodic table. Ge has been plotted with a different symbol to emphasize that the principal axis has changed from the [011] or [0$\bar{1}$1] direction to the [100] direction. Dashed lines drawn as visual aid only.

that was first pointed out by Jensen *et al.*[4] In a given row of the periodic table, the strength of the electric-quadrupole interaction is roughly constant, while the asymmetry parameter η increases with solute-solvent valence difference Z'. The extent to which this generalization characterizes the data is shown in Fig. 1. Figure 1 plots η versus excess charge for the row beginning with Zn, for which only the $Z'=1$ and $Z'=4$ solutes have been measured, and for the row beginning with Cd, for which all members through $Z'=4$ have been measured. The Ge data have been plotted with a different symbol to emphasize the fact that the increase in η with increasing Z' has gone so far in this case as to change the principal axis of the efg from within the cubic plane {i.e., either [011] or [0$\bar{1}$1] for the nucleus at (011)} to perpendicular to the cubic plane { to the [100] direction for the (011) nucleus}. On the other hand, for charged impurities, e^2qQ/h is 2 MHz ± 25% for $Z'=1,\ldots,4$.

III. DISCUSSION

The long-range and oscillatory nature of the screening charge around a metallic impurity was first explicated by Friedel,[5] and applied to the nuclear-magnetic-resonance problem by Kohn and Vosko.[6] The connection between theory and experiment is made by a set of scattering phase shifts, n_l, $l=0, 1, 2, \ldots$, which have been determined semiempirically in a variety of ways. In order to facilitate comparison with the work of Jensen[4] *et al.*[4] we follow them in calculating the efg $V_{zz}\equiv eq$ from the self-consistent screening potential of Alfred and Van Ostenberg[7] using the phase shifts of Hurd and Gordon.[8] The appropriate formulas are reproduced by Jensen, Nevaid, and Williams,[4] and we have used the same value of the core-enhancement factor $\alpha=25.6$ as do Jensen *et al.*, as calculated by Kohn and Vosko.[6] It should be emphasized that the screening potential of Alfred and Van Ostenberg[7] is a function only of the distance from the impurity, so that the electric field gradient in this model is axially symmetric, with the principal axis the radius vector from the impurity to the copper site in question. This result is correct for the next-neighbors [(100) type relative to impurity] for symmetry reasons but, as we have emphasized above, is quite wrong for nearest neighbors for which the model fails to make any statement at all about one of the striking systematic features of the data—the variation of the asymmetry parameter η as a function of solute valence. We have tabulated (Table IV) the field gradients for nearest and next-nearest neighbors calculated using the phase shifts of Hurd and Gordon and the screening potential of Alfred and Van Ostenberg. The calculations are to be compared with columns 4 and 5 of Table II of Jensen *et al.*, which they largely reproduce. Slight differences in the numbers may reflect small differences in the lattice parameter and wave vector, for which we used $a=6.82$ a.u. and $k_F=0.715$ a.u. Gold is not included in the table since Hurd and Gordon[8] did not calculate phase shifts for this impurity. (In-

TABLE IV. $|q|$ in 10^{24} cm^{-3}, for nearest and next-nearest neighbors to the listed impurities, calculated as explained in text. Connection with experimental values made by the conversion factor 10^{24} cm^{-3} is equivalent to $e^2qQ/2h$ = 2.62 MHz.

Impurity	First neighbor (theory)	Second neighbor (theory)	First neighbor (expt.)	Second neighbor (expt.)
Zn	0.123	−0.00766	0.75[a]	0.0292[b]
Ge	0.70	−0.189	0.74[c]	<0.3[c]
Cd	0.136	−0.0179	0.58[a]	0.157[a]
In	0.381	−0.0538	0.85[c]	<0.3[c]
Sn	0.625	−0.1405	0.88[c]	0.442[c]
Sb	0.995	−0.31	0.992[c]	0.664[c]
Ag	−0.102	0.023	0.218[a]	0.181[a]

[a]This paper. [b]Redfield, Ref. 2. [c]Jensen *et al.* Ref. 4.

deed, they remark that their calculations is not valid for homovalent solutes, so the results for Ag in Cu are presumably also invalid.)

Two features of the consequences of the theory are perhaps not adequately emphasized by the table. The first-neighbor theoretical-field-gradient magnitude is strongly charge dependent, while the experimental values are not. The second-neighbor theoretical gradients are also charge dependent, and the experimental gradients, although lacking Ge and In, seem to depend more strongly on charge. But the quantitative agreement is just as poor as for the first neighbors, being relatively good only for the case of Sb, where $Z'=4$. We have calculated (unpublished) the gradient out to distances from the impurity which include the seventh shell, and find the field gradients to be too small to explain the measured wipeout numbers. That is, the Alfred–Van Ostenberg potentials with the Hurd–Gordon phase shifts are adequate to explain the data in neither the near nor asymptotic regions, whereas simpler approaches,[9] such as Kohn–Vosko, have been more successful in the asymptotic region.

ACKNOWLEDGMENTS

We wish to express our appreciation to Professor Paul Flinn and John Rayne for their excellent advice on sample preparation, and to Professor Larry Vassamillet for the electron-microprobe analysis of the samples.

*Work supported by National Science Foundation Grant No. GP-17559. From Ph.D. thesis of George Schnakenberg, Jr., 1971.

†Present address: United States Bureau of Mines, 4800 Forbes Ave., Pittsburgh, Pa. 15213.

[1]T. J. Rowland, Phys. Rev. **119**, 900 (1960).

[2]A. G. Redfield, Phys. Rev. **130**, 589 (1963).

[3]R. T. Schumacher and George Schnakenberg, Jr., Solid State Commun. **7**, 1735 (1969).

[4]B. L. Jensen, R. Nevald, and D. L. Williams, J. Phys. F **2**, 169 (1972).

[5]J. Friedel, Philos. Mag. 43, 153 (1952).

[6]W. Kohn and S. H. Vosko, Phys. Rev. **119**, 912 (1960).

[7]L. C. R. Alfred and D. O. Van Ostenberg, Phys. Lett. A **26**, 27 (1967).

[8]C. M. Hurd and E. M. Gordon, Phys. Chem. Solids **29**, 2205 (1968).

[9]K. Tompa, G. Grüner, A. Janossy, and F. Toth, Solid State Commun. **7**, 697 (1969).

PHYSICAL REVIEW B VOLUME 7, NUMBER 6 15 MARCH 1973

Lattice Thermal Conductivity in High-Concentration Mixed Crystals*

J. K. Flicker and P. L. Leath
Department of Physics, Rutgers, The State University, New Brunswick, New Jersey 08903
(Received 2 August 1972)

The lattice thermal conductivity in high-concentration harmonic isotopically disordered mixed crystals is calculated within the coherent-potential approximation from the appropriate Kubo formula using the energy current operators of Hardy. The infrared divergence in harmonic systems is eliminated by restriction to finite systems and, in a three-dimensional case, by adding an anharmonic phonon-phonon scattering term. Numerical calculations are performed in one, two, and three dimensions with nearest-neighbor forces for a linear chain, a simple square lattice, and a simple cubic lattice, respectively. In one and two dimensions, comparisons with the computer experiments of Payton *et al.* show qualitative agreement with the concentration dependence of the thermal conductivity at all concentrations although the overall magnitude is larger by factors of about 10.8 and 5.4, respectively. It is observed that low-frequency resonant modes considerably decrease the thermal conductivity.

I. INTRODUCTION

There has been considerable discussion in the literature of the thermal conductivity of disordered systems by several quite distinct approaches, most of them in one-dimensional systems. A useful test of various analytical approaches has been provided by Payton *et al.*,[1] who performed computer experiments on one- and two-dimensional isotopically disordered lattices. They used the classical equations of motion of the lattice atoms to calculate the local energy density and hence the energy flow at one end of their system when the other end of their system was allowed to be in contact with particles having a Maxwellian distribution of velocities. They plotted the thermal conductivity versus concentration of the two isotopic species throughout the concentration range.

Recently, several groups have concerned themselves with the dependence of the lattice thermal conductivity κ of a disordered, harmonic, one-dimensional chain on its number of atoms N. For